

Anomalies in magnetoresistance and in the bulk modulus for ferromagnetics with four-spin exchange interaction on the Kondo lattice

This article has been downloaded from IOPscience. Please scroll down to see the full text article.

2006 J. Phys.: Condens. Matter 18 6859

(<http://iopscience.iop.org/0953-8984/18/29/023>)

View [the table of contents for this issue](#), or go to the [journal homepage](#) for more

Download details:

IP Address: 129.252.86.83

The article was downloaded on 28/05/2010 at 12:24

Please note that [terms and conditions apply](#).

Anomalies in magnetoresistance and in the bulk modulus for ferromagnetics with four-spin exchange interaction on the Kondo lattice

S S Aplesnin¹ and N I Piskunova²

¹ L V Kirenskii Institute of Physics, Siberian Branch of the Russian Academy of Sciences, Krasnoyarsk, 660036, Russia

² M F Reshetneva Aircosmic Siberian State University, Krasnoyarsk, 660014, Russia

E-mail: apl@iph.krasn.ru

Received 14 February 2006, in final form 14 June 2006

Published 6 July 2006

Online at stacks.iop.org/JPhysCM/18/6859

Abstract

The temperature dependence of resistivity and the bulk modulus are calculated on the Kondo lattice, with ring exchange between localized spins, using the spin-polaron and adiabatic approximation. Peak and zero values of the bulk modulus as functions of temperature and concentration are determined below the temperature of the transition to the paramagnetic state. The effects of the nearest order between transverse spin components and a value of the ring exchange between localized spins on magnetoresistivity are estimated.

(Some figures in this article are in colour only in the electronic version)

1. Introduction

Recent interest in manganites has been stimulated by the presence of the large magnetoresistance effect in these materials, which makes them possible candidates for applications in spintronic devices. A number of previous works showed the variety of magnetic phases, phase transitions and phenomena that depend on doping concentration, temperature, type of ion $Re = La, Pr, Nd$ and the doping element used $A = Ca, Sr, Ba$, etc see the reviews [1, 2]. A ferromagnetic dielectric becomes a ferromagnetic metal with colossal magnetoresistance near T_c for $x > 0.2$. Previous simulations explored the competition between the double exchange induced ferromagnetism and the antiferromagnetic super exchange [3]. Millis *et al* [4] showed that the electron–phonon coupling resulted from the Jahn–Teller splitting of a Mn^{3+} ion and this affects the transport properties of manganites. Measurements of the specific heat indicate the anomalous softening of a lattice arising from the T^3 -term of the specific heat in a sufficiently wide x region ($0.1 < x < 0.3$) [5]. However, this softening does not have much influence on the rhombohedral–orthorhombic transition of a crystal. The strong coupling with a lattice can induce the four-spin exchange interaction (A) with the value

$AS^4 \sim \frac{1}{Ma^2} (\frac{\nabla J}{\theta_D})^2$, where θ_D is the Debye temperature ($\theta_D = 320\text{--}450$ K) [6], $M \sim 10^{-22}$ g, $a \sim 410^{-10}$ m, S varies from $S = 2$ to $3/2$ depending on the doping concentration, ∇J is the spin–lattice coupling constant. The four-spin exchange interaction resulting from the exchange by virtual phonons is $A \sim 0.1$ meV for $\frac{\nabla J}{\theta_D} \sim 0.03$. This interaction can cause modification of the magnetic structure, for example, the formation of strip structures on a square lattice [7]. Also, it can change the temperature dependence of magnetization and the spin–spin correlation function and can open the gap in the spin wave spectrum [8]. With increasing values of the four-spin exchange, the magnetic phase transition type changes from continuous to discontinuous.

In this paper, the lattice effect is considered as a result of the spin–lattice interaction, and the magnetoresistance effect is described in terms of the interaction of current carriers with localized spins on the Kondo lattice using spin polarons as charge carriers. The temperature and concentration ranges where the metal–insulator transition occurs and the change in the elastic modulus are determined as functions of the spin polaron band population and the four-spin interaction. We will show the relevant dependence of resistance on the spin–spin correlation function for nearest transverse spin components. The model proposed here differs from the double-exchange model, in which the hopping of electrons over e_g levels of Mn ions leads to the formation of ferromagnetic exchange, while hopping over t_{2g} states leads to the antiferromagnetic exchange between localized electrons. We assume that the motion of charged carriers takes place in the oxygen system and electron spins are polarized by the ordering of manganese spins through the hybridization of oxygen and manganese ions. According to the x-ray diffraction data [9], the weights of the $3d^5 L^1$ and $3d^6 L^2$ states are approximately equal to 41% and 9%, respectively which correspond to one- and two-hole states. These states are located in the gap; they can be treated as impurity bands near the chemical potential and can be described by the model of nearly free electrons. As applied to manganites, our model suggests that the substitution of the bivalent ion Sr^{2+} or Ca^{2+} for the trivalent La^{3+} ion leads to an increase in the hole concentration in oxygen ions.

2. Model and calculation method

Spin-polaron excitations can be calculated in the framework of the Kondo-lattice model using the method proposed in [10]. The Hamiltonian has the form

$$\begin{aligned}
 H &= H_0 + H_1 + H_2, \\
 H_0 &= \sum_{\mathbf{r}, \mathbf{g}} t_{\mathbf{g}} a_{\mathbf{r}+\mathbf{g}, \sigma}^\dagger a_{\mathbf{r}, \sigma} = \sum_{\mathbf{k}} \varepsilon_{\mathbf{k}} a_{\mathbf{k}, \sigma}^\dagger a_{\mathbf{k}, \sigma}, \\
 H_1 &= J \sum_{\mathbf{r}, \sigma_1, \sigma_2} a_{\mathbf{r}, \sigma_1}^\dagger S_{\mathbf{r}}^\alpha \hat{\sigma}_{\sigma_1, \sigma_2}^\alpha a_{\mathbf{r}, \sigma_2}, \\
 H_2 &= -\frac{1}{2} \sum_{\mathbf{r}, \mathbf{g}} I(\mathbf{g}) S_{\mathbf{r}+\mathbf{g}}^\alpha S_{\mathbf{r}}^\alpha - \frac{1}{2} \sum_{\mathbf{i}, \mathbf{j}, \mathbf{k}, \mathbf{l}} A_{\mathbf{i}, \mathbf{j}, \mathbf{k}, \mathbf{l}} (S_{\mathbf{r}_i}^\alpha S_{\mathbf{r}_j}^\alpha) (S_{\mathbf{r}_k}^\alpha S_{\mathbf{r}_l}^\alpha) - \sum_{\mathbf{r}} h S_{\mathbf{r}}^z
 \end{aligned} \tag{1}$$

where the summation is made over the cubic lattice sites, I is the exchange interaction between the nearest neighbours, A is the four-spin interaction between spins situated in the square vertexes, for example, $A_{1234}((S_1 S_2)(S_3 S_4) + (S_1 S_3)(S_2 S_4))$, $a_{\mathbf{k}, \sigma}^\dagger$ is the creation operator for an electron with the spin index $\sigma = \pm 1$, H_1 is the Hamiltonian of the s–d interaction and $\hat{\sigma}^\alpha$ are the Pauli matrices with $\alpha = x, y, z$, h the external magnetic field. Let us write the equations of motion for the Green’s functions describing the motion of an electron over oxygen ions. The electron spin interacts with magnetically ordered spins of manganese ions. Using the random phase approximation, we close the system of equations for the Green’s functions $\langle\langle a_{\mathbf{r}, \sigma} | a_{\mathbf{r}, \sigma}^\dagger \rangle\rangle$

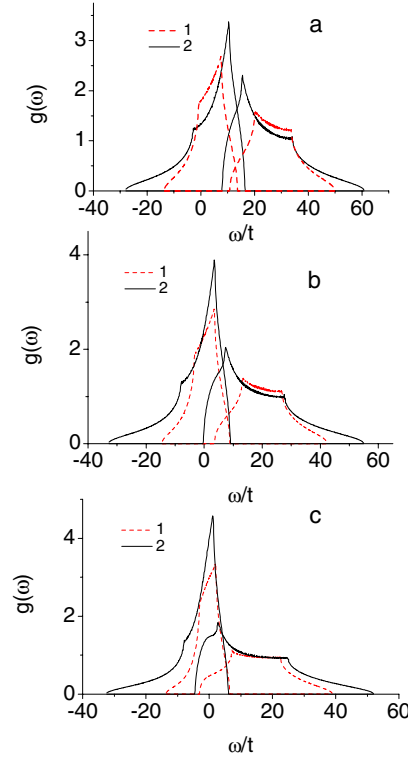


Figure 1. The density of states $g(\omega)$ of spin-polaron excitations for $A/I = 0.15$, $J/t = 9$, $n = 0.2$ (a), $n = 0.4$ (b), $n = 0.6$ (c) and $T/T_c = 0.4$ (1—dotted line), $T/T_c = 1$ (2—solid line).

and $\langle\langle b_{\mathbf{r},\sigma} | a_{\mathbf{r},\sigma}^\dagger \rangle\rangle$, where, $b_{\mathbf{r}\sigma} = S_{\mathbf{r}}^\alpha \hat{\sigma}_{\sigma,\sigma_1}^\alpha a_{\mathbf{r},\sigma_1}$, $\alpha = x, y$. These equations have the form:

$$\begin{aligned}
 (\omega - \varepsilon_{\mathbf{k}})G_{\mathbf{k}}^1 &= 1 + \frac{J}{2}G_{\mathbf{k}}^2, \\
 (\omega - e_{\mathbf{k}})G_{\mathbf{k}}^2 &= J(1 + m - 2nm)G_{\mathbf{k}}^1, \\
 G_{\mathbf{k}}^1 &= \langle\langle a_{\mathbf{k},\sigma} | a_{\mathbf{k},\sigma}^\dagger \rangle\rangle; & G_{\mathbf{k}}^2 &= \langle\langle b_{\mathbf{k},\sigma} | a_{\mathbf{k},\sigma}^\dagger \rangle\rangle \\
 \varepsilon_{\mathbf{k}} &= \varepsilon_{\mathbf{k}}^0 + \frac{Jm}{4} - \mu, \\
 \varepsilon_{\mathbf{k}}^0 &= -2t(\cos k_x + \cos k_y + \cos k_z), \\
 e_{\mathbf{k}} &= 2z_1 c \varepsilon_{\mathbf{k}}^0 + J\left(\frac{m}{2} + n\right) + \frac{mz_1}{2}I + A\frac{z_2 m^3}{2} + mh - \mu, \\
 n &= \langle a_{\uparrow}^\dagger a_{\uparrow} + a_{\downarrow}^\dagger a_{\downarrow} \rangle.
 \end{aligned} \tag{2}$$

Here $b_{\mathbf{k},\sigma}$, $a_{\mathbf{k},\sigma}$ and $G_{\mathbf{k}}$ are the Fourier transforms of the corresponding single-node operators and Green's functions, $c = \langle S_{\mathbf{r}}^x S_{\mathbf{r}+\mathbf{g}}^x + S_{\mathbf{r}}^y S_{\mathbf{r}+\mathbf{g}}^y \rangle$ is the spin–spin correlation function for transverse spin components, z_1 and z_2 are the numbers of the nearest and next-to-nearest neighbours, respectively, $m = \langle S^z \rangle$ is magnetization. All the energies are measured using the chemical potential μ . The excitation spectrum has the form

$$\omega_{1,2}(\mathbf{k}) = \frac{1}{2} \left[\varepsilon_{\mathbf{k}} + e_{\mathbf{k}} \pm \sqrt{(\varepsilon_{\mathbf{k}} - e_{\mathbf{k}})^2 + J^2 \left(\frac{1+m}{2} - nm \right)} \right]. \tag{3}$$

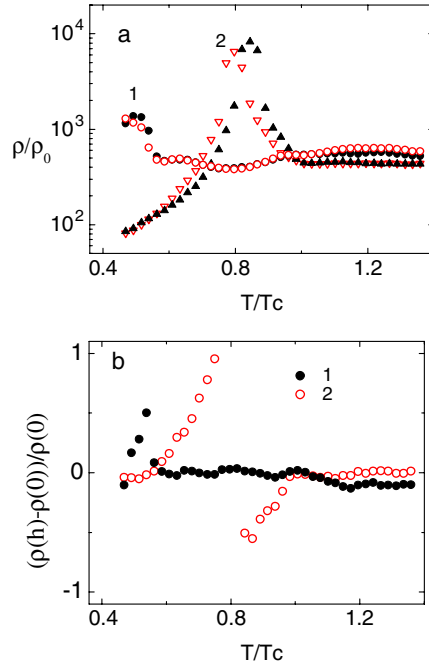


Figure 2. Resistivity ρ/ρ_0 (a) and magnetoresistivity $(\rho(h) - \rho(0))/\rho(0)$ (b) versus normalized temperature calculated in zero magnetic field (black symbol) and in the field $h/I = 0.3$ (white symbol) at different parameters of the sd interaction $J/t = 3(1), 6(2)$, $n = 0.3$, $A/I = 0.15$.

The chemical potential is calculated self-consistently for a given electron concentration n ,

$$n = \frac{1}{N} \sum_{\mathbf{k}} \int d\omega f(\omega) \frac{1}{\pi} \text{Im} G^1, \quad (4)$$

where $f(\omega) = (\exp(\omega/T) + 1)^{-1}$. The summation is made over 8×10^6 points in the first Brillouin zone. Here we analyse the effect of magnetic ordering on transport properties. To simplify the problem we consider the magnetic system in the adiabatic approximation. Magnetization and spin–spin correlations are calculated by the Monte Carlo method on the lattice $18 \times 18 \times 18$ with 28 000 MC/spin for different values A/I by using Hamiltonian H_2 . The typical exchange integral value is $I \sim 1$ meV [11]. Conductivity σ is calculated using the Kubo–Greenwood formula [12]

$$\sigma = \sigma_0 \sum_{\sigma} \sum_{\mathbf{k}} \int d\omega \left(-\frac{\partial f(\omega)}{\partial \omega} \right) A_{\sigma}^2(\mathbf{k}, \omega) \quad (5)$$

where $A_{\sigma}(\mathbf{k}, \omega) = -(1/\pi) \text{Im} G_{\sigma}(\mathbf{k}, \omega)$ is the spectral Green's function, σ_0 is the constant characterizing the conductivity dimension.

According to the calculation of the electron density functional LDA + U , the gap width for the Mn–O charge transfer in LaMnO_3 [13] is $(\varepsilon_p - \varepsilon_d) \sim 3.2$ eV. The Mn–Mn electron orbitals do not overlap directly; the overlap integral of the wavefunction between Mn and O ions is $t(pd\sigma) = -1.99$ eV, $t(pd\pi) = 1.1$ eV and $t(pp\sigma) = 0.7$ eV, $t(pp\pi) = -0.16$ eV [14] for O–O overlapping. Electron excitations are localized on the manganese ions due to the large charge gap and the Coulomb interaction, and nonstoichiometry facilitates the formation of holes with higher mobility in the oxygen subsystem.

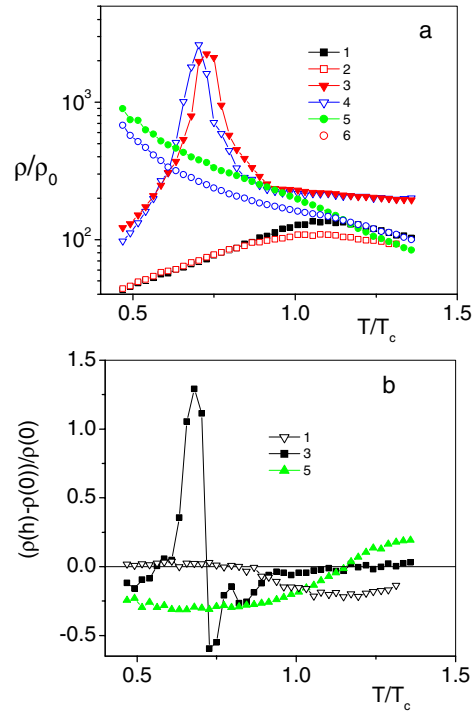


Figure 3. Resistivity ρ/ρ_0 (a) and magnetoresistivity $(\rho(h) - \rho(0))/\rho(0)$ (b) versus normalized temperature calculated in zero magnetic field (1, 3, 5) (black symbol) and in the field $h/I = 0.3$ (2, 4, 6) (white symbol) at different concentrations $x = 0.2$ (1, 2), 0.4(3, 4), 0.6(5, 6), $J/t = 9$, $A/I = 0.15$.

3. Discussion

The electron interaction with localized spins forms the quasigap in the density of states of electron excitations that depends on concentration and on the value of the spin–spin correlation function for transverse spin components. The band splits into two subbands; in one of them electron spins are directed upwards and in the other they are directed downwards. The qualitative understanding of the temperature-dependent resistivity caused by a spin polaron, is based on the assumption that spin polarons are scattered on magnons. For fully polarized spin polarons, the scattering decreases with lowering of temperature as the number of magnons decreases. A partially polarized electron having spin up with weight (W_1) and spin down with (W_2) loses more energy because of the update of a part of the localized spins including the area $T \rightarrow 0$. It results in a resistivity rise with decreasing temperature.

The main contribution to the transport properties is given by the spin polarons possessing energy close to the chemical potential $\mu - k_B T_c < \omega < \mu + k_B T_c$, where T_c is the Curie temperature. Therefore, it is important to estimate the density of states $g(\omega)$ at the chemical potential. $g(\omega)$ are plotted in figure 1 for different concentrations of band filling. At low concentrations the chemical potential lies inside the lower subband in the wide temperature range $T < T_c$, whereas at high concentrations it shifts to the region where the bands overlap. At some sd interaction and concentration parameters the chemical potential shifts from the lower band to the upper one at $T^* < T_c$ (figure 1) with the conservation of the long range ferromagnetic order. As a result, metallic-type conductivity changes into semiconductor-type,

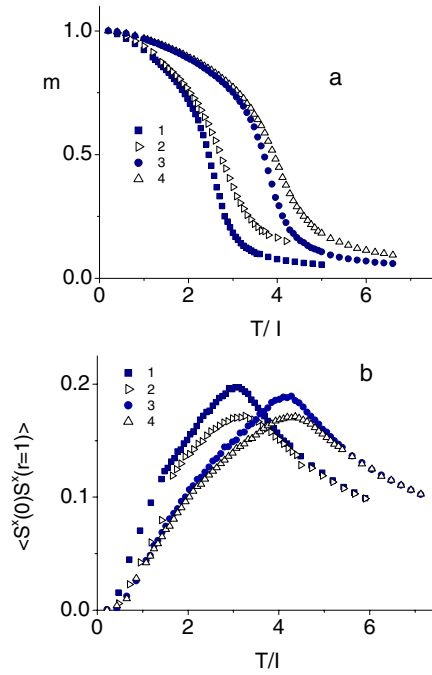


Figure 4. Magnetization (m) (a) and spin–spin correlation function $\langle S^x(0)S^x(r = 1) \rangle$ (b) versus temperature at different parameters of ring exchange $A/I = 0.15(1, 2), 0.3(3, 4)$ and at magnetic fields $h/I = 0(1, 3), h/I = 0.3(2, 4)$.

and the resistivity maximum is observed at $T \approx T^*$ (figures 2, 3). This behaviour becomes clear from analysis of the spectrum of spin-polaron excitations and the density of states $g(\omega)$. Upon cooling, the chemical potential level moves into the van Hove region in the lower band and lies near the bottom of the upper band $\omega_2 \rightarrow 0$. The polaron velocity decreases sharply in the case, $v_k = (\frac{1}{h})\Delta_k\omega_1(k) \rightarrow 0$ or the mobility of the spin polaron tends to zero $\mu \sim \frac{\partial^2\omega_1(k)}{\partial k_\alpha\partial k_\beta} \rightarrow 0$. Since conductivity is proportional to the polaron velocity at the chemical potential $\sigma \sim v_\mu(k)$, this behaviour gives rise to a singularity in the $\rho(T)$ dependence.

The external magnetic field increases the magnetization and decreases the spin–spin correlation function (figure 4). So the ratio of the spin–spin correlation function for transverse spin components to magnetization is equal to 0.17($h = 0$), 0.14($h/I = 0.3$) at $T/T_c = 0.5$ and 0.29($h = 0$), 0.22($h/I = 0.3$) at $T/T_c = 0.75$. The excitation spectrum expression (3) includes the term $e_k \sim \langle S^\alpha(0)S^\alpha(r = 1) \rangle \varepsilon_k^0$ which varies with the bandwidth versus the external magnetic field and temperature. A small variation of the magnetization value forced by the sd interaction leads to a chemical potential shift and to modification of the spectrum of spin-polaron excitations. Temperature dependences of resistivity calculated for zero and non-zero magnetic fields are presented in figures 2 and 3. As one can see in the figures, the resistivity maximum displacement towards low temperatures changes the sign of the magnetoresistance.

The disappearance of the spin–spin correlations $\langle S^\alpha(0)S^\alpha(r = 1) \rangle \rightarrow 0$ leads to decreasing values of ρ and $(\rho(h) - \rho(0))/\rho(0)$ (figure 5). The appearance of an additional scattering channel gives rise to the parameters characterizing kinetic properties. Also, it must be taken into account that the four-spin interaction modifies the magnetoresistivity effect. Resistivity and magnetoresistivity are shown in figure 6 for different parameters of the four-

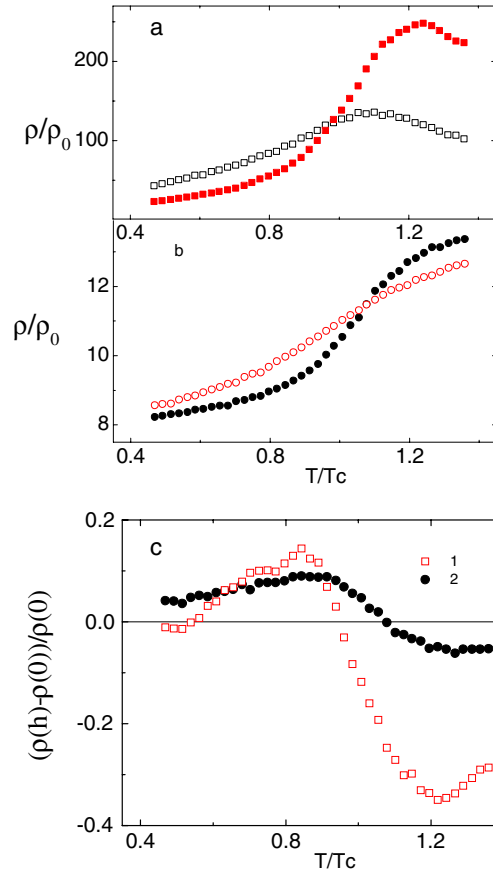


Figure 5. Resistivity ρ/ρ_0 (a), (b) and magnetoresistivity $(\rho(h) - \rho(0))/\rho(0)$, $n = 0.2(1), 0.3(2)$ (c) versus normalized temperature calculated in zero magnetic field (black symbol) and in the field $h/I = 0.3$ (white symbol) without taking into consideration the spin-spin correlation function $\langle S^x(0)S^x(r=1) \rangle = 0$ for $J/t = 9$, $n = 0.2$ (a), 0.3 (b), $A/I = 0.15$.

spin exchange. The best fit to the experimental data $\text{La}_{0.7}\text{Ca}_{0.3}\text{MnO}_3$ [15] is observed at $A/K = 0.15$. The four-spin interaction results in a sharper magnetization decrease and in a rise in the spin-spin correlation function at $T < T_c$. As a result, the changes in temperature behaviour of $m(T)$, $\langle S^\alpha(0)S^\alpha(r=1) \rangle(T)$ enhanced by the sd interaction modify the density of states of spin-polaron excitations and the temperature dependence of resistivity. The two-peak shape in the zero field resistivity arises due to a maximum of the effective mass value $\sigma \sim 1/m_{\text{eff}}$ that is observed in special cases: chemical potential lies at the bottom of the upper band and crosses the van Hove singularity of the lower band ($T < T_c$) or the van Hove singularities of the lower and upper bands are situated in the vicinity of the chemical potential ($T > T_c$). The external magnetic field shifts $\mu \rightarrow \mu - mh$ also as four-spin interaction $\mu \rightarrow \mu - 0.5A_z m^3$ and as a result the effective mass value decreases and the mobility of the spin polaron goes up.

The presence of the strong electron-phonon interaction in a perovskite manganite material is confirmed by dramatic softening of the sound velocity and elastic modulus near the paramagnetic-ferromagnetic phase transition [16]. The results of the calculation of density $\langle n \rangle$ versus chemical potential μ show the jump in density at a certain value of μ depending on

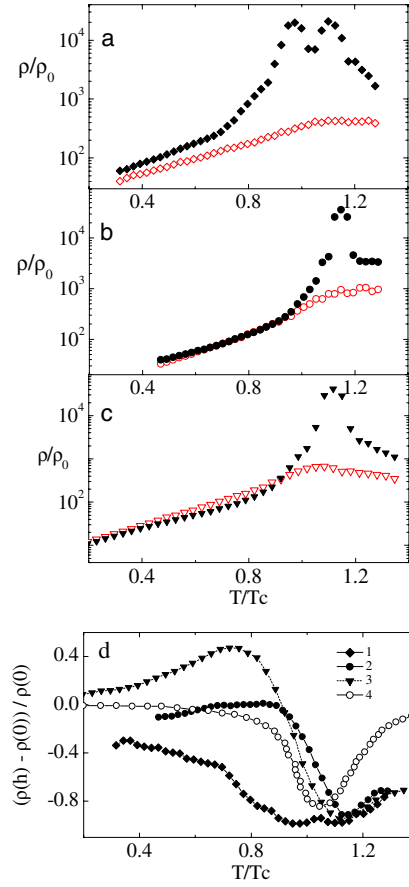


Figure 6. Resistivity ρ/ρ_0 at $A/I = 0$ (a), 0.15 (b), 0.3 (c) and magnetoresistivity $(\rho(h) - \rho(0))/\rho(0)$ (d) versus normalized temperature calculated in zero magnetic field (black symbol) and in the field $h/I = 0.3$ (white symbol) at different parameters of the four-spin interaction $A/I = 0(1)$, 0.15(2), 0.3(3), $J/t = 9$, $n = 0.3$, experimental data (4) [15].

the space dimension, for example, $\langle n \rangle \sim 0.15$ for 2D [17]. Similarly to the phase separated state (PS), ferromagnetic polarons can form extended structures. Polarons are spread over a distance equal to a few lattice constants rather than being close to each other, like in a PS. Let us express the bulk modulus of an electron gas using the thermodynamic properties. The bulk modulus is

$$\begin{aligned}
 B &= -V \frac{\partial p}{\partial V}; & p &= -\frac{\partial F}{\partial V}; & V &= \frac{N}{n}; & \frac{\partial V}{\partial n} &= -\frac{N}{n^2}; \\
 F &= E - TS = \sum_{\mathbf{k}} [f(\omega(\mathbf{k}))(\omega(\mathbf{k}) - 2k_B T \log(f(\omega(\mathbf{k}))))] \\
 B &= \frac{n^2}{N} \left[\frac{\partial^2 F}{\partial^2 n} n + 2 \frac{\partial F}{\partial n} \right]_{T,N}.
 \end{aligned} \tag{6}$$

The simulated temperature dependences of the normalized bulk modulus are shown in figure 7. The bulk modulus for polaron gas changes in sign around the Curie temperature and has a small value at low temperatures for $n = 0.2$. This concentration is in good agreement with the critical concentration $n \sim 0.18$ obtained by using the double-exchange model with a

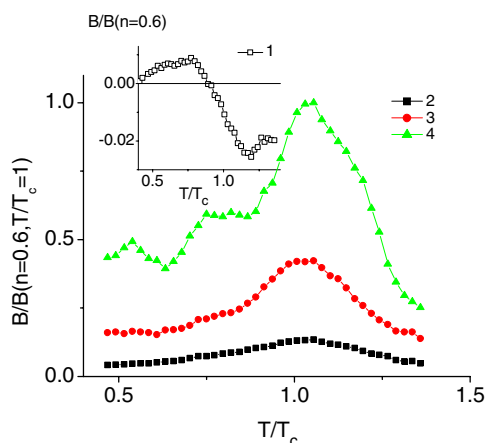


Figure 7. The bulk modulus normalized by the value of B determined at $n = 0.6$, $T/T_c = 1$ versus temperature T/T_c at $n = 0.2$ (inset), 0.3 (2), 0.4 (3), 0.6 (4) for $J/t = 9$, $A/I = 0.15$.

localized spin, where the compressibility coefficient becomes negative at $T \rightarrow 0$ [18]. This clarifies the origin of temperature anomalies in structural deformation $\text{La}_{1-x}\text{Ca}_x\text{MnO}_3$. For $x < 0.2$ the Bragg peaks indicate the re-entrance into the high-temperature pseudocubic phase at $T/T_c \simeq 0.4$, whereas for $x = 0.2$ the peaks are not resolved [19]. A similar anomaly is observed in Sr-doped samples [20], which corresponds to the sharp change in two of the three Mn–O distances [21]. Moreover, in Sr-doped compounds, new Bragg reflections occur below $T < T^*$ that are forbidden in $Pbnm$ symmetry [22]. They are related to the polaron ordering, which has been revealed in low-doping $\text{La}_{0.85}\text{Sr}_{0.15}\text{MnO}_3$ compounds by neutron scattering studies [22]. The volume magnetostriction in $\text{La}_{1-x}\text{Sr}_x\text{MnO}_3$ has a maximum at the Curie point for the sample with $x = 0.3$, while for the semiconducting sample with $x = 0.1$ it is negative at $T < T_c$ and tends to zero at $T \sim T_c$ [23]. At high concentrations, the bulk modulus becomes maximal at the ferromagnetic–paramagnetic transition and can make a considerable contribution to the strong magnetostriction, which is observed in the optimally doped manganites [24], and to the anomalies of the volume thermal expansion in Ca-doped compounds at the metal–insulator transition [25] that have been revealed by x-ray and neutron power diffraction studies.

4. Conclusion

The spin–phonon interaction expressed by the ring exchange between localized spins causes sign reversal of the magnetoresistance from negative to positive below the Curie temperature. The spin–spin correlations between the transverse localized spin components lead to an increase in the resistivity and magnetoresistivity effects. Temperature resistivity maxima and magnetoresistivity in the magnetic long range order at $T < T_c$ cause a shift in the chemical potential located in the fully polarized subband to the partially spin polarized subband at heating or cooling. With decreasing temperature, the bulk modulus changes sign from negative to positive near the Curie temperature and becomes small at low temperatures and low concentrations ($n \simeq 0.2$). In doped manganites, spin polarons make their contribution to the anomalies in the magnetostriction and in the volume thermal expansion in the vicinity of the Curie temperature.

References

- [1] Nagaev E L 1996 *Phys. Usp.* **39** 781
Kagan M Yu and Kugel K I 2001 *Phys. Usp.* **44** 553
- [2] Salamon M B and Jaime M 2001 *Rev. Mod. Phys.* **73** 583
- [3] De Gennes P G 1960 *Phys. Rev.* **118** 141
- [4] Millis A J, Littlewood P B and Shraiman B I 1995 *Phys. Rev. Lett.* **74** 5144
- [5] Okuda T, Asamitsu A, Tomioka Y, Kimura T, Taguchi Y and Tokura Y 1998 *Phys. Rev. Lett.* **81** 3203
- [6] Coey J M D, Viret M, Ranno L and Ounadjela K 1995 *Phys. Rev. Lett.* **75** 3910
- [7] Sandvik A W, Daul S, Singh R R P and Scalapino D J 2002 *Phys. Rev. Lett.* **89** 247201
- [8] Aplesnin S S 2003 *Phys. Lett. A* **313** 122
Aplesnin S S 2004 *Phys. Lett. A* **333** 446
- [9] Sarma D D, Rader O, Kachel T, Chainani A, Mathew M, Holldack K, Gudat W and Eberhardt W 1994 *Phys. Rev. B* **49** 14238
- [10] Barabanov A F, Maksimov L A and Mikheenkov A V 2001 *JETP Lett.* **74** 328
- [11] Feinberg D, Germain P, Grilli M and Seibold G 1998 *Phys. Rev. B* **57** R5583
- [12] Nagai K, Momoi T and Kubo K 2000 *J. Phys. Soc. Japan* **69** 1837
- [13] Chainani A, Mathew M and Sarma D D 1993 *Phys. Rev. B* **47** 15397
- [14] Mahadevan P, Shanthi N and Sarma D D 2001 *Phys. Rev. B* **54** 11199
- [15] Coey J M D, Viret M and von Molnar S 1999 *Adv. Phys.* **48** 167
- [16] Zhu C and Zheng R 1999 *J. Phys.: Condens. Matter* **11** 8505
Seiro S, Salva H R, Saint-Paul M, Ghilarducci A A, Lejay P, Monceau P, Nunez-Regueiro M and Sulpice A 2002 *J. Phys.: Condens. Matter* **14** 3973
- [17] Dagotto E, Hotta T and Moreo A 2001 *Phys. Rep.* **344** 1
- [18] Kagan M Yu, Khomskii D I and Mostovoy M V 1998 *Preprint cond-mat/9804213*
- [19] Biotteau G, Hennion M, Moussa F, Rodriguez-Carvajal J, Pinsard L, Revcolevschi A, Mukovskii Y M and Shulyatev D 2001 *Phys. Rev. B* **64** 104421
- [20] Kawano H, Kajimoto R, Kubota M and Yoshizawa H 1996 *Phys. Rev. B* **53** R14 709
- [21] Pinsard L, Rodriguez-Carvajal J and Moudou A H 1997 *Physica B* **234-236** 856
- [22] Yamada Y, Hino O, Nohdo S, Kanao R, Inami T and Katano S 1996 *Phys. Rev. Lett.* **77** 904
- [23] Koroleva L I, Abramovich A I, Demin R V and Michurin A V 2001 *Low Temp. Phys.* **27** 293
- [24] Abramovich A I, Koroleva L I and Michurin A V 2002 *JETP* **95** 917
Zheng R K, Zhu C F, Xie J Q and Li X G 2000 *Phys. Rev. B* **63** 024427
- [25] Radaelli P G, Cox D E, Marezio M, Cheong S-W, Schiffer P E and Ramirez A P 1995 *Phys. Rev. Lett.* **75** 4488